doi: 10.15407/ujpe62.07.0615

I. KUPCHAK, N. SERPAK

V.E. Lashkaryov Institute of Semiconductor Physics, Nat. Acad. of Sci. of Ukraine
(41, Nauka Ave., Kyiv 03028, Ukraine; e-mail: kupchak@isp.kiev.ua)

ELECTRONIC AND MAGNETIC PROPERTIES OF SPINEL Co_3O_4 (111) SURFACE IN GGA + U APPROXIMATION

PACS 73.20.At, 75.70.Rf

The atomic structure and electronic properties of the spinel Co_3O_4 (111) surface are calculated within the methods of density functional theory. Possible types of the surface are analyzed, and their formation energies are calculated. Electron states formed at the surface by broken bonds are studied in detail, and their partial density of states is calculated. It is shown that, unlike the bulk of spinel, its surface has nontrivial magnetic properties, because Co atoms acquire an additional magnetic moment under near-surface conditions.

K e y w o r d s: spinel, cobalt oxide, magnetic surface structure.

1. Introduction

Tricobalt tetraoxide Co_3O_4 known as cobalt spinel is a semiconductor of the p-type with the energy gap width E_g varying from 1.1 to 1.65 eV according to various literature data [1]. It is widely used in a lot of catalytic reactions. In particular, when being doped with lithium atoms, this substance acquires the ability to reversely intercalate lithium ions, which allows it to be used as a cathode in lithium-based current sources [2]. The application of nanostructured cobalt spinel in this case makes it possible to lower the charge-discharge overvoltage for $Li - O_2$ batteries [3]. An important factor at that is the surface orientation of nanocrystals: the largest effect is observed in the case of (111) surface, and the smallest one for the (100) surface. Interesting and promising are also the applications of cobalt spinel as low-temperature CO sensors [4, 5], a catalyst of N_2O decomposition [6] and NH_3 oxidation [7], as well as in other domains [8–11].

At the crystallization, Co_3O_4 creates a cubic structure of normal spinel AB_2O_4, in which cobalt ions with two different oxidation degrees, Co^{2+} and Co^{3+}, are located at the sites with the crystal environment characterized by the tetrahedral (A) or octahedral (B) symmetry, respectively [1], so that the chemical formula can be written in the form $Co^{2+}Co_2^{3+}O_4^{2-}$. The geometrical structures of sites A and B, as well as the splitting of cobalt ion d-orbitals at them, are schematically shown in Fig. 1. Hence, in the presence of a tetrahedral crystalline field, the fivefold degenerate d-orbital of Co^{2+} ion becomes split into two levels: the doubly degenerate e_g level and the triply degenerate t_{2g} one. According to the Hund rule, three electrons fill t_{2g} orbitals, and four electrons occupy the e_g orbital, which is lower by energy. Similarly, the crystalline field in a vicinity of the Co^{3+} ion has octahedral symmetry. Therefore, the splitting of d-orbitals results in six paired electrons located on the ground level t_{2g}, leaving the level e_g empty. The Hund rule is not obeyed in this case, because the splitting magnitude is substantial and amounts to 2.4 eV [12]. As a result, the Co^{2+} ions have a permanent magnetic moment, whereas the Co^{3+} ones have no such magnetic properties. Taking only sublattice A into consideration, the system becomes magnetically ordered at a low enough temperature. In this case, each Co^{2+} ion in sublattice A is surrounded by four neighbors with oppositely directed spins, thus forming an antiferromagnetic state [13].

For typical well-studied spinels such as Fe_3O_4 [14], the magnetic properties are associated with the exchange A–B interaction between the ions at the tetrahedral and octahedral sites, whereas the A–A interaction is negligibly small. However, it is the A–A interaction that dominates in spinel Co_3O_4. This interaction turns out extremely strong owing to the indirect exchange through an intermediate Co^{3+} ion at octahedral site B, with the corresponding magnetic moment of Co^{2+} ions amounting to $3.02\mu_B$. These anti-

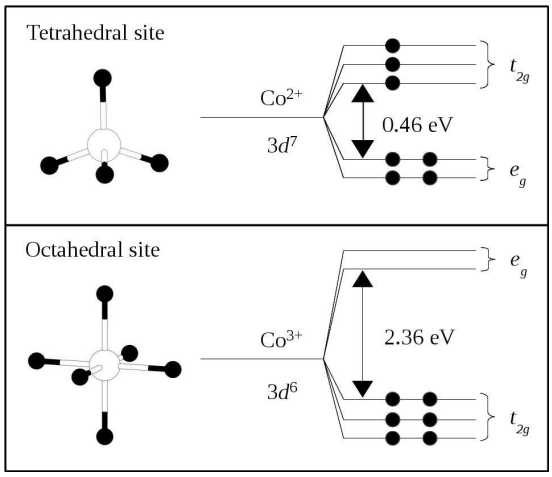

Fig. 1. Splitting of d-states of cobalt ions in the tetrahedral and octahedral crystalline fields

ferromagnetic properties survive only below the Néel temperature $T_N \approx 40$ K. At higher temperatures, the substance becomes paramagnetic [13].

Theoretical researches of the spinel surface were carried out in works [15–17]. In those works, the density functional method was used to calculate the electronic characteristics and the conditions of thermodynamic stability for the surfaces (100), (110), and (111). One of the important aspects of theoretical calculations is the study of the magnetic parameters of spinel, because, as follows from the group theory, this substance cannot be antiferromagnetic. This conclusion is associated with the fact that the group of spatial symmetry $Fd\bar{3}m$, which describes the structure of normal cubic spinel (in particular, Co_3O_4), does not contain corresponding magnetic groups (Shubnikov groups) [18]. At the same time, in experimental and other theoretical researches, this substance reveals antiferromagnetic properties at low temperatures, so that there arise difficulties in putting the results of theoretical group analysis into agreement with other results.

One of the possible explanations of this discrepancy is the lowering of the spinel lattice symmetry from cubic to tetragonal (or trigonal) at low temperatures due to the spontaneous magnetostriction [19]. As a result, the crystal structure is described by a certain group of spatial symmetry that already contains magnetic groups corresponding to antiferromagnetic states. However, as far as we know, at present, this issue has not been completely resolved.

As was already mentioned above, cobalt spinel has catalytic properties that manifest themselves owing to the features of the spinel surface. Moreover, in some applications, the surface orientation is a crucial factor, because only at some orientations – this is mainly the surface (111) – a catalytic reaction is possible, as was shown in work [3]. The other important factors are the geometrical structure and the ionic composition of the surface. In addition, taking into account that this substance is a p-type semiconductor, it becomes also promising for electronics, because it simultaneously posesses both the electronic and magnetic properties. Therefore, the aim of this work was to study the atomic, electron, and magnetic structures of the surface (111) of cobalt spinel Co_3O_4.

The structure of the work is as follows. In Section 2, a model of the surface and the calculation procedure used throughout the work are described. In Section 3, the calculation results obtained for the free energy of the surface of various types are presented. In Section 4, the results of calculations obtained for the geometrical, electron, and magnetic structures of the spinel surface (111) are quoted. Conclusions are made in Section 5.

2. Model and Calculation Procedure

The crystalline structure of cobalt spinel in the direction [111] can be described as a sequence of cobalt atomic layers separated by monolayers of oxygen atoms. Every cobalt layer can contain only Co^{3+} ions or both Co^{2+} and Co^{3+} ions. Respectively, the surface (111) can be formed in various ways, depending on which layer is chosen to be at the surface. Therefore, in this work, we examined all the cases: the B-terminated surface formed by Co^{3+} ions and the A-terminated surface formed by Co^{2+} and Co^{3+} ions. Furthermore, the surface can be both clean (terminated by cobalt ions; these are surfaces A and B) and oxidized (terminated by oxygen ions; these are surfaces AO and BO). As was discussed above, Co^{2+} ions have a magnetic moment. Therefore, one should expect that, near the surface, the situation should not change. However, if the surface is formed by Co^{3+} ions, which have no magnetic moment in the spinel bulk, variations in the crystalline field symmetry can result in the appearance of new properties. Generally speaking, ions

at the surface can have a charge state different from the corresponding values in the bulk, so it would be reasonable to introduce special notations for them for all surface types. However, we formally use the notations Co^{2+} and Co^{3+} for all cobalt ions, including the surface ones, in order to not overload the text with a redundant number of notations.

The calculations were carried out within the density functional theory (DFT) and generalized gradient approximation (GGA) with account of spin (SGGA), as implemented in the Quantum-Espresso software package [20]. Ultrasoft Perdew–Burke–Ernzerhof pseudopotentials [21], which involve six valence electrons for oxygen and nine valence electrons (including the 3*d*-shell) for cobalt, were used. Moreover, we added an on-site Coulomb correction in the Hubbard model [22] for 3*d* states of cobalt, $U = 3.5$ eV. The integration over the Brillouin zone was carried out with the use of a Γ-centred $4 \times 4 \times 1$ mesh of special points in the **k**-space, which were generated following the Monkhorst–Pack scheme [23] and the Methfessel–Paxton scheme [24] with a smearing parameter of 0.005 Ry.

The preliminary calculations showed that the growth of the *k*- point mesh dimension to $6 \times 6 \times 1$ gives rise to a change of the surface free energy within the limits of ≈ 2 meV/Å^2. However, the duration of calculations increases substantially at that. Therefore, the choice of the $4 \times 4 \times 1$ mesh was a compromise. All calculated quantities confidently coincided at the kinetic energy maximum equal to 35 Ry. However, we increased the corresponding value to 40 Ry in order to avoid possible difficulties associated with the application of ultrasoft pseudopotentials in GGA + U calculations and to accelerate the convergence of iteration procedures.

In order to calculate the surface energy and other properties of such systems, we considered the unit cells in the initial structure obtained by "cutting" out a definite part from bulk spinel, which would satisfy periodic conditions in two directions. In turn, the atomic structure of bulk spinel was calculated by applying the symmetry operations of space group $Fd\bar{3}m$ to the basis atoms with the coordinates Co^{2+} $(0, 0, 0)$, Co^{3+} $(5/8, 5/8, 5/8)$, and O^{2-} $(3/8, 3/8, 3/8)$ reckoned in units of the experimental lattice constant value $a = 8.084$ Å. The obtained unit cells were supercells of the hexagonal structure with the lattice constant $a_{\text{hex}} = 5.716$ Å and containing five cobalt layers separated by oxygen layers, with the surface layers having the identical structure (termination), as is schematically illustrated in Fig. 2 (layers *1* and *5*). Such symmetric structures are nonstoichiometric. However, their electrostatic dipole moment equals zero (or is close to zero). The presence of the latter can considerably affect the electronic properties of the surface. Furthermore, the calculation procedure assumed the presence of translational symmetry in three dimensions. Therefore, we added a vacuum gap 12 Å in thickness to the unit cell in order to exclude the Coulomb interaction between the layers. In turn, this operation lowered the symmetry to C_{3v}.

In order to verify the model, we calculated a similar structure containing nine cobalt layers. No essentially new properties in comparison with the 5-layer structure were revealed.

The obtained unit cells were optimized over all internal coordinates, by using the Broyden–Fletcher–Goldfarb–Shanno (BFGS) method, which is realized in the software package Quantum-Espresso. The optimization was carried out until the forces acting on the atoms reached values less than 10^{-4} a.u. The geometrical optimization was performed without taking the spin into account, whereas the calculation of electronic parameters included the spin variable.

3. Geometrical Structure and the Free Energy of the Surface

In general, during the geometrical optimization, all examined surface types kept C_{3v} symmetry. In all cases, ions in the inner layer (layer *3* in Fig. 2) practically did not change their positions. However, in other layers, the lengths of Co–O bonds are changed, mainly due to the displacements of cobalt ions in the external layer. At the oxidized surfaces, the largest variation of bond lengths with respect to the lengths of corresponding bonds in bulk spinel was observed in the near-surface layers of the tetrahedral surface and amounted to about 0.2%. At the same time, changes in layers *2* and *3* were even smaller, and the oxidized octahedral surface did not undergo appreciable modifications during the optimization.

For clean surfaces, the bond lengths are changed more strongly. In particular, the bond lengths in the external layer increases by about 0.8% at the octahedral surface and, on the contrary, diminished by about 5.9% at the tetrahedral one. Moreover, in the structure of a clean surface with octahedral termi-

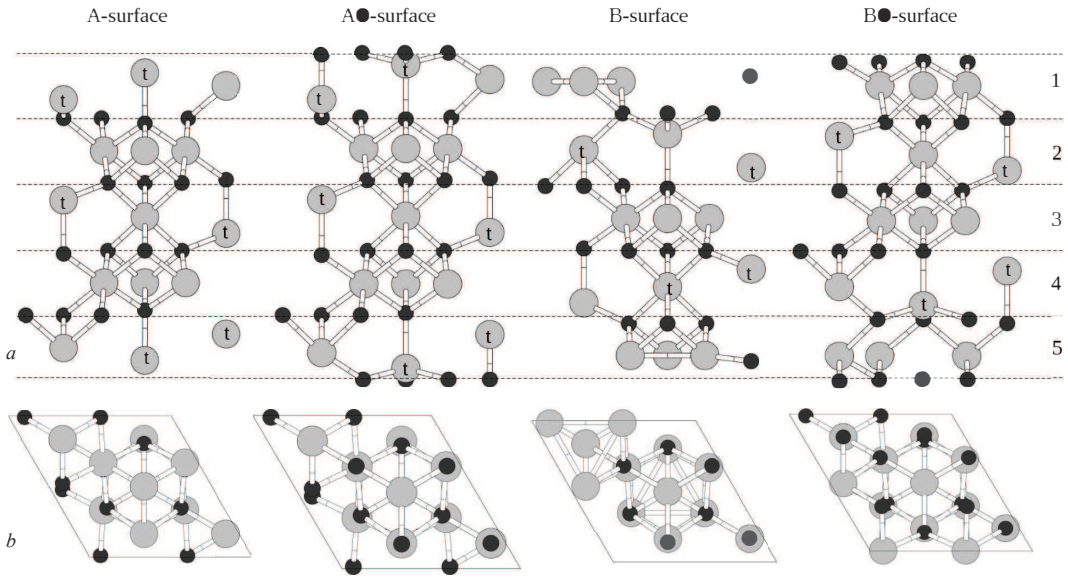

Fig. 2. Atomic structure of a model supercell at the cobalt spinel surface Co_3O_4 (111): side view (a); top view in the direction [111] (b). Large circles correspond to cobalt atoms, the letter t marks Co^{2+} ions, small circles correspond to oxygen atoms

nation, one of the oxygen ions that sepatates cobalt layers *1* and *2* breaks its chemical bond with the Co^{2+} ion in layer *2*, shifted by 1.3 Å toward the surface, and thus became built-in into the cobalt surface layer. Accordingly, the surface Co^{3+} ions change their positions in the plane (111), so that the distance between them decreases by about 12% (from 2.91 to 2.55 Å). Since the unit cells were chosen to be symmetric, the same took place with the ions in layers 4 and 5, as is shown in Fig. 2.

Under the thermodynamic equilibrium conditions, the most stable structure of the surface is a structure that is characterized by the minimum of free energy [25]

$$\lambda = \frac{1}{2S}[E_{Co_3O_4} - N_{Co}\mu_{Co} - N_O\mu_O],$$

where N_{Co} and N_O are the numbers of cobalt and oxygen, respectively, atoms in the system; μ_{Co} and μ_O are their chemical potentials; and S is the surface area. Here, the total energy of the system $E_{Co_3O_4}$ calculated in the DFT approximation is used as the Gibbs free energy. Under the equilibrium conditions, the chemical potential of a structural unit of spinel equals $\mu_{Co_3O_4} = 3\mu_{Co} + 4\mu_O$, which imposes conditions on the determination of the chemical potentials for cobalt and oxygen. In turn, μ_{Co} and μ_O can be determined, if we assume that the structure is in a gas medium (i.e. it is condensed from a gaseous state), which can be oxygen-rich or oxygen-lean. The oxygen-rich environment means that, at a low enough temperature, the oxygen condensation will take place. Therefore, the chemical potential μ_O is determined as half the total energy of an oxygen molecule: $\mu_O = E_{O_2}/2$. In this case, the chemical potential of cobalt can be determined as $\mu_{Co} = [E_{Co_3O_4} - 2E_{O_2}]/3$. Under the oxygen-lean conditions, the cobalt condensation will take place. Therefore, μ_{Co} can be determined as the total energy of a cobalt atom in the bulk: $\mu_{Co} = E_{Co}^{bulk}$, and the corresponding chemical potential of oxygen equals $\mu_O = [E_{Co_3O_4} - 3E_{Co}]/4$.

Hence, what remains to calculate is the total energies of an oxygen molecule and unit cells of bulk cobalt and spinel. To calculate the total energy of a single oxygen molecule, we put it into a cubic lattice with a constant of 25 Å in order to avoid the Coulomb interaction between neighbor molecules as a result of the translational symmetry. The long-range part of this interaction was taken into account, by using the Martyna–Tuckerman method [26]. On the other hand, in the calculations of bulk cobalt, we took a hexagonal unit cell with the lattice constants $a = 2.51$ Å and $c = 4.1$ Å, which contained two atoms. For bulk spinel, a primitive face-centered cell

containing two Co^{2+}, four Co^{3+}, and eight O^{2-} ions was used. The integration over the Brillouin zone was carried out using a single Γ point in the k-space for oxygen, and a $12\times12\times12$-mesh of k-points for cobalt and spinel. The values of other calculation parameters were left the same as in Section 2.

Taking all the aforesaid into account, we carried out the geometrical optimization of the systems over all internal variables. As a result, we obtained the total energy of the system and the corresponding chemical potentials. The calculated surface free energies for all types of surface termination are quoted in Table 1. As one can see, both in the oxygen-rich and oxygen-lean media, the smallest value of the surface free energy was obtained for the oxygen-terminated A surface, although, in general, the process of surface formation is endothermal for all surface types.

It should be noted that the calculations, in which PBE pseudopotentials [20] are used, give an overestimated value for the binding energy of an oxygen molecule, whereas the account of the Hubbard correction for cobalt allows the total energy and, accordingly, the chemical potential to be calculated more precisely. This fact explains a considerable difference between the magnitude of surface energy for O-terminated surfaces in various media and the corresponding magnitude for clean surfaces.

In experimental works, Meyer *et al.* [27] studied Co_3O_4 (111) films obtained by depositing cobalt onto the substrate Ir(100) with a simultaneous supply of O_2, which actually corresponds to the condensation from an oxygen-rich environment. The measurements were carried out under the conditions of ultrahigh vacuum. The STM images clearly demonstrate a hexagonal structure corresponding to the plane (111), whereas LEED spectra testify to the film termination by a layer of Co^{2+} ions, with the thickness of this layer being almost half as large as in the bulk owing to a substantial shortening of Co–O bonds. Therefore, under ultrahigh vacuum conditions, the formation of the surface layer of the film Co_3O_4 (111) terminated by Co^{2+} ions is energetically preferable.

Furthermore, in work [27] and in other experimental works [28, 29], it was shown that the surface Co^{2+} ions are the most active in the oxidation processes of CO molecules on the Co_3O_4 (111) surface. At the early exposure stage, CO molecules first bind to Co^{2+} ions and afterward weakly bind between the sites of A sublattice. Those results, as a whole, confirm our conclusion that the most stable type of the Co_3O_4 (111) surface is the surface with tetrahedral termination, irrespectively of whether it is clean or oxidized. Nevertheless, we should repeat that those calculations are based on the application of PBE pseudopotentials, which are not so good for an oxygen molecule as for spinel and cobalt.

4. Electronic and Magnetic Properties of the Surface

In a bulk material, every atom is surrounded by a correct crystal environment providing the saturation of chemical bonds. At the surface, the coordination environment is violated, which results in the appearance of dangling bonds. The latter, in turn, can create local energy levels in the energy gap, the so-called surface states.

In this section, we will consider the energy structure and the nature of such surface states. For this purpose, we calculated the partial density of states (PDOS) cosidering the contribution of only surface atoms: cobalt or cobalt and oxygen, depending on the surface type. For comparison, we also calculated the PDOS in bulk spinel. In this case, we accounted for the electron states of cobalt ions that lie in the plane (111) and form layers with the given ionic composition: only Co^{3+} ions (similarly to the B-terminated surface) or cobalt ions of both types, Co^{2+} and Co^{3+} (similarly to the A-terminated surface). The results obtained are depicted in Fig. 3.

It should be noted that all PDOSs were calculated making allowance for the spin. However, the figure demonstrates the sum of the densities of states of electrons with different spins. In addition, to avoid a redundant specification, the Gaussian smearing of lines with a half-width of 100 meV was used here. The energies of all PDOSs are reckoned from the correspond Fermi levels, whose values, for convenience, were put equal to zero in the figure. As one can see, the PDOSs in bulk spinel in both A and B layers

Table 1. **Formation energies for surfaces of various types in the approximations of O-rich and O-lean environment**

Surfaces of types	A, meV/Å^2	AO, meV/Å^2	B, meV/Å^2	BO, meV/Å^2
O-rich	295	62	323	115
O-lean	245	122	263	175

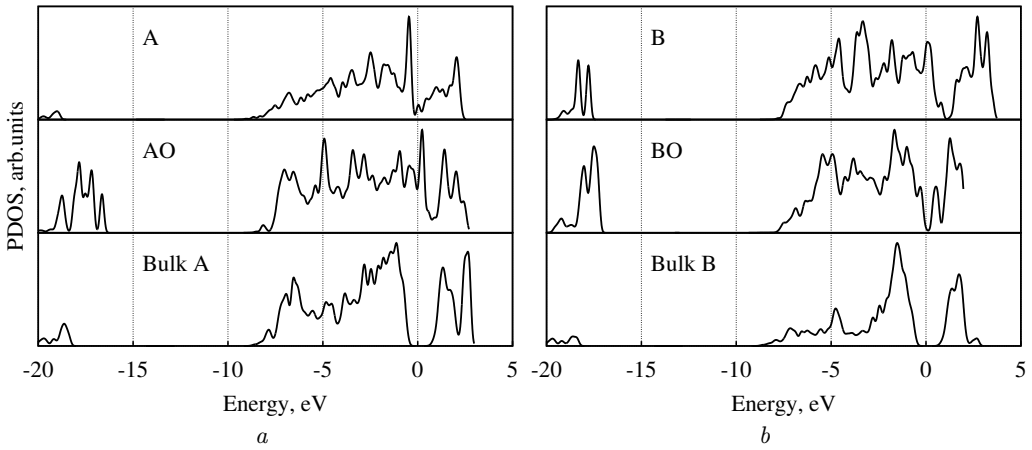

Fig. 3. Partial density of states for cobalt ions: at tetrahedral surface A (a) and octahedral surface B (b) calculated for the clean surface, O-terminated surface, and the corresponding plane of bulk spinel (from top to bottom)

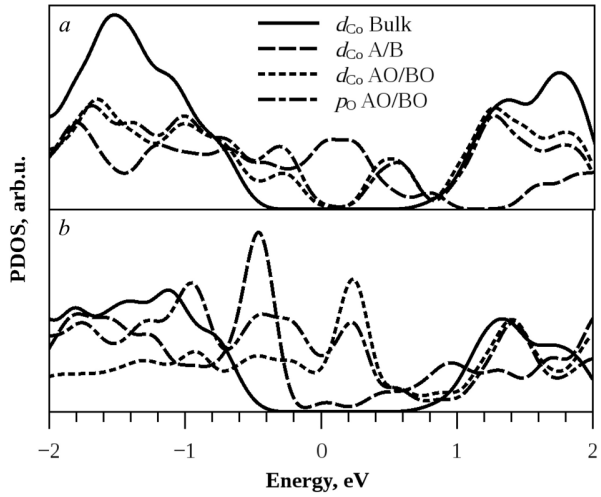

Fig. 4. Partial density of states projected on d-orbitals of cobalt ions and p-orbitals of oxygen ions: octahedral surface B (a), tetrahedral surface A (b)

demonstrate a pronounced forbidden gap of the width $E_g \approx 1.1$ eV. This value is comparable with the energy gap width in bulk spinel Co_3O_4 obtained in the calculations of work [1], although it is a little smaller than its experimental value.

The spectra of surfaces with AO and BO terminations also demonstrate a forbidden gap. However, in this case, the gap contains separate peaks located near the Fermi level.

For systems with a clean A- or B-terminated surface, much larger number of such peaks are observed. They are stronger delocalized and almost fill the forbidden gap. Such delocalization of electron states results in the "partial metallization" of the surface. This result is confirmed by the fact that one-electron energy levels obtained by solving the Kohn–Sham equation are characterized by noninteger occupation numbers. In Fig. 4, the partial contributions of d-orbitals of cobalt ions and p-orbitals of oxygen ions are shown in detail for all surface types. All other orbitals (s-states of cobalt and oxygen) make a contribution to the total density of states near -18 eV; therefore, they are not shown in the figure. One can see that, in the case of clean A- and B-terminated surfaces, extra peaks in the forbidden gap are formed by d-orbitals of cobalt ions.

It is natural that the external atoms in the structures have dangling bonds. Therefore, such states in the energy gap have a "surface-induced" character. At the oxidized surfaces (A- and B-terminated), external cobalt atoms have a regular crystal environment, whereas oxygen ions are surface ones. Therefore, in this case, "surface" states are formed by dangling oxygen p-orbitals. Nevertheless, even in this case, the d-orbitals of cobalt ions also form additional peaks in the forbidden gap.

It is clear that the appearance of surface states results in a redistribution of the density of states as a whole and can affect the magnetic properties of the surface. To verify this statement, we calculated the magnetic moments of the surface cobalt and oxygen ions proceeding from the analysis of the electron state population on the basis of the Löwdin method.

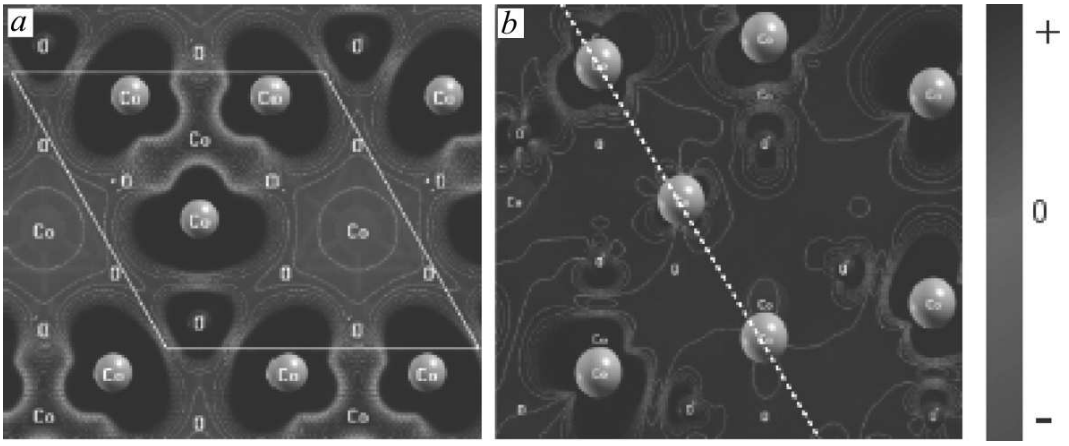

Fig. 5. Spin density distributions (the difference between the charge densities for electrons with oppositely directed spins, $\rho(\uparrow) - \rho(\downarrow)$): in the plane passing through surface Co^{3+} ions in the B-terminated structure (a); in the plane passing through surface ions in the A-terminated structure (b)

In Table 2, the maximum values of the magnetic moments calculated for all surface types and bulk materials are quoted. As one can see, unlike the bulk spinel case, all surface cobalt ions have a nonzero magnetic moment. The Co^{2+} ions at the A- and AO-terminated surfaces have a magnetic moment close to the corresponding moment in the bulk. The Co^{3+} ions are nonmagnetic in the bulk, but, at the surface B, they have a magnetic moment close to that of Co^{2+} ions and, at the surface BO, a magnetic moment that is substantially smaller, but also nonzero. Furthermore, oxygen ions at the AO- and BO-surfaces also have nonzero magnetic moments, which indicates the polarization of their p-orbitals, probably as a result of the chemical bond disbalance.

Figure 5, a demonstrates the spin density distribution calculated for the surface B in the plane (111) that passes through three surface Co^{3+} ions and one O^{2-} ion. White lines mark a two-dimensional unit cell. From the analysis of the total density of states, one can see that the charge is mainly localized at the sites, so that this compound has a high degree of ionicity. The main contribution to the density of ionic charges is made by the cobalt states with the positive spin orientation (blue color), whereas the red color corresponds to the negative orientation of Co^{2+} ions in the lower layer. The green color corresponds to the spin-nonpolarized charge density (or the charge absence). This spin distribution corresponds to the parallel orientation of the spins of surface atoms; hence, the surface has ferromagnetic properties. It is important to note that the oxygen ion is also polarized here, which is indicated by the blue color in its vicinity.

Figure 5, b demonstrates the distribution of spin density calculated for the surface A in the plane that passes through three surface Co ions and perpendicularly to the surface. One can see that the surface Co^{2+} ions are polarized in this case, but the spin orientation is antiparallel. A region of the charge with negative spin polarization is also observed around the Co^{3+} ion (in the upper left corner), which testifies that the ion has a magnetic moment. Accordingly, this surface is antiferromagnetic. It should be noted that Co^{3+} ions in the inner layers (along the dashed line in the figure) remain nonmagnetic. Their magnetic moment diminishes as the distance to the surface grows. For layer 3, this moment becomes negligibly small, which is confirmed by the absence of red- or blue-colored regions near it.

As was indicated above, cobalt ions Co^{3+} are nonmagnetic in bulk spinel, whereas Co^{2+} ions have a nonzero magnetic moment as a result of the indirect exchange interaction through the intermediate Co^{3+}

Table 2. **Magnetic moments of cobalt and oxygen ions for various surface types (in μ_B units)**

Ions	A	AO	B	BO	Bulk
Co^{3+}	1.77	2.27	0.43	0.70	0.0
Co^{2+}	2.45		2.51		2.59
O^{2-}			0.35	0.35	

ion in the octahedral B site. Therefore, we may assume that a regular crystal environment for cobalt ions is formed not only by the nearest oxygen ions, but also by the nearest neighbors from the corresponding A or B sublattice. It is evident that the absence of the nearest Co^{2+} or Co^{3+} ion will result in the A-A energy change or the emergence of the A-B superexchange interaction between the neighbor cobalt atoms. For instance, in the case of B surface, the angle Co^{3+}–O–Co^{3+} created by the surface cobalt atoms and the nearest internal oxygen atoms amounts to 87°. According to the Goodenough–Kanamori–Anderson (GKA) rules, the 90°-angle provides a stable ferromagnetic superexchange interaction between the neighbor "magnetic" atoms, because, as was shown in work [30], a deviation of the angle from this value cannot cardinally transform the magnetic interaction into the antiferromagnetic one.

The angles formed with the use of the oxygen ion that lies in the same plane with surface cobalt ions amount to 128°, but the GKA rules are not accurately formulated for such angles. In the optimized bulk spinel, the angle Co^{3+}–O–Co^{3+} equals 94°, which is also close to 90°. However, cobalt ions at B sites have no magnetic moments. That is why the superexchange interaction between them is absent. For the oxidized BO surface, the angles Co^{3+}–O–Co^{3+} with internal oxygen ions amount to 92° and to about 100° for external oxygen ions. In these cases, the ferromagnetic interaction should be expected.

Concerning the A-terminated surface, the normal superexchange A-A interaction evidently dominates here, because the surface Co^{3+} ions, which now possess a magnetic moment, form a Co^{3+}–O–Co^{2+} angle of about 123°, for which the GKA rules are not determined, and the cobalt ions in the lower layer are not magnetic. The situation is similar for the oxidized AO surface, because the Co^{3+}–O–Co^{2+} angles with internal and external oxygen ions amount, respectively, to 119° and 137°.

In order to confirm or discard our conclusions made on the basis of GKA rules, we calculated the total energy of the A and B surfaces at various spin orientations of surface Co^{3+} ions. It turned out that the B surface has the lowest energy in the ferromagnetic state, although the energy difference between its ferro- and antiferromagnetic states is rather small and amounts to about 4 meV. The total energy of surface A practically does not depend on the spin orientation of an Co^{3+} ion, and its minimum value corresponds to the antiferromagnetic state. In this case, the energy difference between the ferro- and antiferromagnetic states is a little larger and amounts to 8 meV. For the oxidized surfaces, similar calculations were not carried out. However, since the GKA gives correct results in our calculations, one should expect that the magnetic properties of the AO- and BO-terminated surfaces would be similar to the properties of A- and B-terminated ones. Therefore, both the A- and AO-terminated surfaces have antiferromagnetic properties provided by the superexchange A-A interaction, whereas the B- and BO-terminated surfaces are ferromagnetic owing to the appearance of the superexchange B-B interaction.

5. Conclusions

Cobalt spinel Co_3O_4 is a semiconductor substance, which demonstrates antiferromagnetic properties below the Néel temperature $T_N \approx 40$ K. Those magnetic properties in the bulk material are provided by the superexchange interaction between neighbor Co^{2+} ions. Near the surface, the crystal environment of ions is violated both near and apart from them, which results in a modification of magnetic properties of this surface depending on the type of its termination. In this work, we have carried out complex calculations of the atomic structure and electronic and magnetic properties for the Co_3O_4 (111) surfaces of various types. The results obtained can be summarized as follows:

i) the surface including Co^{2+} ions (these are the surfaces A and AO) has the lowest surface energy;

ii) Co^{2+} ions, which have no magnetic moment in bulk spinel, acquire a magnetic moment near the surface; the magnitude of this magnetic moment is comparable with that of Co^{2+} ions;

iii) the A and AO surfaces have antiferromagnetic properties owing to the A-A superexchange interaction, whereas the B and BO surfaces are ferromagnetic owing to the appearance of the additional B-B superexchange interaction.

In general, those conclusions agree with the results of STM and LEED measurements [27]. However, it should be noted that, in the course of the Co_3O_4 deposition onto a substrate under real conditions, the substrate surface is nonideal. Terraces of atomic layers with "steps" at the boundaries will be formed

on it, as well as defects of various kinds, in particular, oxygen vacancies. Some of defects can be removed by the annealing or another post-growth treatment. Generally speaking, the closer the surface structure to the ideal one, the more actively its magnetic properties will manifest themselves.

On the other hand, under certain conditions, magnetic phenomena manifest themselves in cobalt oxide nanocrystals, for which any specific orientation of the surface is quite doubtful. In particular, an interesting manifestation of the surface magnetism of this kind is represented by a modification of magnetic properties of the mixture of zinc oxide (ZnO) powder and cobalt oxide (Co_3O_4) [31,32]. Despite that the former is diamagnetic and the latter paramagnetic (or antiferromagnetic at low temperatures), their mixture reveals ferromagnetism at room temperature. The cited authors explained this phenomenon by a variation in the charge state of surface ions at octahedral sites, $Co^{3+} \to Co^{2+}_{oct}$, under the influence of the electrostatic interaction between oxides. In this case, the magnitude of d-orbital splitting decreases a little (Fig. 1), and the Hund rule is satisfied, which gives rise to the appearance of a nonpaired electron in the ground t_{2g} state and, accordingly, to the new $Co^{2+}_{oct} - O - Co^{2+}$ superexchange interaction. This phenomenon is observed not only for ZnO, but also for other oxides, such as SiO_2, Al_2O_3, and others, with the Co_3O_4 content in the mixture not exceeding 1%.

Another domain, where the surface magnetism can manifest itself, includes diluted magnetic semiconductors (DMSs), such as ZnO : Co. Doping zinc oxide with cobalt atoms in high concentrations is known to result in the appearance of a secondary phase in the form of spinel Co_3O_4 or $ZnCo_2O_4$, which reveals itself, in particular, in Raman spectra [33]. Depending on where the new phase is formed – at the surface or in the bulk – either an oriented Co_3O_4 surface or the case, described above, of the electrostatic interaction between two oxides, respectively, can be realized. Hence, the presence of the surface of the secondary phase Co_3O_4 in DMSs can be one of the origins of ferromagnetism in real crystals.

The work was supported in the framework of The Science for Peace and Security Programme (NATO grant NUKR.SFPP 984735) and the program HORIZON2020 (RISE project CoExAN GA644076).

1. A. Walsh, S.-H. Wei, Y. Yan, M.M. Al-Jassim, J.A. Turner, M. Woodhouse, B.A. Parkinson. Structural, magnetic, and electronic properties of the Co–Fe–Al oxide spinel system: Density-functional theory calculations. *Phys. Rev. B* **76**, 165119 (2007).
2. E. Meza, D. Alburquenque, J. Ortiz, J.L. Gautier. Lithium cobalt spinel oxide: A structural and electrochemical study. *J. Chil. Chem. Soc.* **53**, 1494 (2008).
3. D. Su, S. Dou and G. Wang. *Sci. Rep.* **4**, 5767 (2014).
4. X. Xie, Y. Li, Z.-Q. Liu, M. Haruta, W. Shen. Single crystalline Co_3O_4 nanocrystals exposed with different crystal planes for Li–O_2 batteries. *Nature* **458**, 746 (2009).
5. Y.-Z. Wang, Y.-X. Zhao, C.-G. Gao and D.-S. Liu. Origin of the high activity and stability of Co_3O_4 in low-temperature CO oxidation. *Catal. Lett.* **125**, 134 (2008).
6. C. Ohnishi, K. Asano, S. Iwamoto, K. Chikama, M. Inoue. Alkali-doped Co_3O_4 catalysts for direct decomposition of N_2O in the presence of oxygen. *Catal. Today* **120**, 145 (2007).
7. K. Schmidt-Szalowski, K. Krawczyk, J. Petryk. The properties of cobalt oxide catalyst for ammonia oxidation. *Appl. Catal. A* **175**, 147 (1998).
8. M. Bajdich, M. Garcia-Mota, A. Vojvodic, J.K. Norskov, A.T. Bell. Theoretical investigation of the activity of cobalt oxides for the electrochemical oxidation of water. *J. Am. Chem. Soc.* **135**, 13521 (2013).
9. H.-J. Kim, J.-H. Lee. Highly sensitive and selective gas sensors using p-type oxide semiconductors: Overview. *Sens. Actuat. B* **192**, 607 (2014).
10. D.R. Miller, S.A. Akbar, P.A. Morris. Nanoscale metal oxide-based heterojunctions for gas sensing: A review. *Sens. Actuat. B* **204**, 250 (2014).
11. *Oxide Materials at the Two-Dimensional Limit,* edited by F.P. Netzer, A. Fortunelli (Springer, 2016).
12. J.S. Griffith. *The Theory of Transition-Metal Ions* (Cambridge Univ. Press, 1971).
13. W.L. Roth. The magnetic structure of Co_3O_4. *J. Phys. Chem. Solids* **25**, 1 (1964).
14. J. Noh, O.I. Osman, S.G. Aziz, P. Winget, J.-L. Bredas. Magnetite Fe_3O_4 (111) surfaces: Impact of defects on structure, stability, and electronic properties. *Chem. Mater.* **27**, 5856 (2015).
15. A. Montoya, B.S. Haynes. Periodic density functional study of Co_3O_4 surfaces. *Chem. Phys. Lett.* **502**, 63 (2011).
16. X.-L. Xu, Z.-H. Chen, Y. Li, W.-K. Chen, J.-Q. Li. Bulk and surface properties of spinel Co_3O_4 by density functional calculations. *Surf. Sci.* **603**, 653 (2009).
17. J. Chen, A. Selloni. Electronic states and magnetic structure at the Co_3O_4(110) surface: A first-principles study. *Phys. Rev. B* **85**, 85306 (2012).
18. J.M. Perez-Mato, S.V. Gallego, E.S. Tasci, L. Elcoro, G. de la Flor, M.I. Aroyo. Symmetry-based computational tools for magnetic crystallography. *Annu. Rev. Mater. Res.* **45**, 217 (2015).
19. Y.E. Kitaev, P. Tronc. Ferromagnetic and antiferromagnetic ordering in the wurtzite-type diluted magnetic semi-

conductors. *Phys. Solid State* **54**, 520 (2012); P. Tronc, private communication.
20. P. Giannozzi, S. Baroni, N. Bonini *et al.* Quantum ESPRESSO: a modular and open-source software project for quantum simulations of materials. *J. Phys. Condens. Matter* **21**, 395502 (2009).
21. J.P. Perdew, K. Burke, M. Ernzerhof. Generalized gradient approximation made simple. *Phys. Rev. Lett.* **77**, 3865 (1996).
22. J. Hubbard. Electron correlations in narrow energy bands. *Proc. R. Soc. London A* **276**, 238 (1963).
23. J.D. Pack, H.J. Monkhorst. "Special points for Brillouin-zone integrations" – a reply. *Phys. Rev. B* **16**, 1748 (1977).
24. M. Methfessel, A.T. Paxton. High-precision sampling for Brillouin-zone integration in metals. *Phys. Rev. B* **40**, 3616 (1989).
25. A. Soon, M. Todorova, B. Delley, C. Stampfl. Thermodynamic stability and structure of copper oxide surfaces: A first-principles investigation. *Phys. Rev. B* **75**, 125420 (2007).
26. G.J. Martyna, M.E. Tuckerman. A reciprocal space based method for treating long range interactions in ab initio and force-field-based calculations in clusters. *J. Chem. Phys.* **110**, 2810 (1999).
27. W. Meyer, K. Biedermann, M. Gubo, L. Hammer, K. Heinz. Surface structure of polar Co_3O_4(111) films grown on Ir(100)-(1x1). *J. Phys.: Condens. Matter* **20**, 265011 (2008).
28. P. Ferstl *et al.* Adsorption and activation of CO on Co_3O_4 (111) thin films. *J. Phys. Chem. C* **119**, 16688 (2015).
29. S.C. Petitto, E.M. Marsh, G.A. Carson, M.A. Langell. Cobalt oxide surface chemistry: The interaction of CoO (100), Co_3O_4 (110) and Co_3O_4 (111) with oxygen and water. *J. Mol. Catal. A* **281**, 49 (2008).
30. W. Geertsma, D. Khomskii. Influence of side groups on 90° superexchange: A modification of the Goodenough–Kanamori–Anderson rules. *Phys. Rev. B* **54**, 3011 (1996).
31. M.S. Martin-González *et al.* A solid-state electrochemical reaction as the origin of magnetism at oxide nanoparticle interfaces. *J. Electrochem. Soc.* **157**, E31 (2010).
32. M.A. García *et al.* Surface magnetism in ZnO/Co_3O_4 mixtures. *J. Appl. Phys.* **107**, 043906 (2010).
33. T.-L. Phan, N.X. Nghia, S.C. Yu. Raman scattering spectra and magnetic properties of polycrystalline $Zn_{1-x}Co_xO$ ceramics. *Solid State Commun.* **152**, 2087 (2012).

Received 25.03.17.
Translated from Ukrainian by O.I. Voitenko

І.М. Купчак, Н.Ф. Серпак

ЕЛЕКТРОННІ ТА МАГНІТНІ ХАРАКТЕРИСТИКИ ПОВЕРХНІ ШПІНЕЛІ Co_3O_4 (111) В НАБЛИЖЕННІ GGA + U

Р е з ю м е

Методом функціонала густини розраховано атомну структуру та електронні властивості поверхні шпінелі Co_3O_4(111). Розглянуто можливі типи поверхні, розраховано вільну енергію їх формування. Детально досліджено електронні стани, що утворюються внаслідок обірваних зв'язків на поверхні, та розраховано їхню парціальну густину. Показано, що на відміну від об'ємної шпінелі, її поверхня володіє нетривіальними магнітними властивостями внаслідок того, що атоми кобальту в умовах поверхні набувають ненульового магнітного моменту.